2021

An Approach to Detach the Thermodynamic Losses of a Reciprocating Compressor

Ernane Silva
TEG/UFSC, Brazil

Thiago Dutra
thiago.dutra@teg.ufsc.br

An Approach to Detach the Thermodynamic Losses of a Reciprocating Compressor

Ernane SILVA[1]*, Thiago DUTRA[2]

[1]TEG Thermofluids Engineering Group, Federal University of Santa Catarina, 89219600, Joinville, SC, Brazil
Phone:+ 55 48 37217307
ernane.silva@teg.ufsc.br

[2]TEG Thermofluids Engineering Group, Federal University of Santa Catarina, 88905120, Ararangua, SC, Brazil
Phone:+ 55 48 999177691
thiago.dutra@teg.ufsc.br

* Corresponding author

ABSTRACT

Due to several incentives for reducing energy consumption worldwide, there is an increasingly demand for high-efficiency compressors for refrigeration systems. During the design stage of a refrigeration compressor, the designer needs to identify the main energy losses so as to propose alternatives to increase the compressor efficiency. The energy losses associated with the compression cycle are typically evaluated from the indicated diagram, which allows an accurate estimate of viscous flow losses through the suction and discharge systems, but no clear identification of piston-cylinder leakage and heat transfer losses. This paper presents a theoretical method to assess the energy losses associated with the compression chamber based on the analysis of the first law of thermodynamics, in which losses are detached into heat transfer, leakage, valve backflow and others. For this purpose, a compressor simulation model based on a transient and lumped formulation of mass and energy conservation equations is applied to the compression chamber and is validated with experimental data. A study case is performed in which the energy losses of a baseline compressor is compared with those of a 4% higher isentropic efficiency compressor. It is concluded that the typical indicated diagram analysis does not allow a clear identification of the benefits that cause the increase of 4% in isentropic efficiency, whereas the approach proposed herein and based on the first law of thermodynamics indicates that the increase of isentropic efficiency is associated with reduction in heat transfer and leakage losses during expansion and discharge processes.

1. INTRODUCTION

Refrigeration and air conditioning systems consume about 17% of the overall electricity used worldwide (Coulomb *et al*., 2015). Many of these systems are based on the vapor compression cycle and the compressor is responsible for most part of the energy consumption. According to Pérez-Segarra *et al*. (2005), the compressor energy losses can be classified as: (i) electrical losses caused mainly by ohmic resistance in the electric motor; (ii) mechanical losses generated by friction in the bearings and; (iii) thermodynamic losses associated with irreversibilities during the compression of the gas. Currently, the thermodynamic and electrical efficiencies of a small reciprocating compressor are around 82-83%, whereas the mechanical efficiency is nearly 91-92% (Diniz *et al*., 2018). Further improvements of compressor performance require the detailed detachment of these energy losses.

The thermodynamic losses are generally assessed via the pressure-volume diagram. Pérez-Segarra *et al*. (2005), for instance, split the compression work in one compression cycle according to its physical sub-processes (suction, compression, discharge, and expansion). They define efficiencies associated with each sub-process taking the ideal (isentropic) compressor as reference. However, due to heating effects and valves closing/opening delays the efficiency associated with the expansion sub-process is generally higher than one and the authors suggest that the compression and expansion processes would be more conveniently expressed by a combined efficiency. Therefore, it is possible to account for three sources of energy losses: (i) underpressure during the suction process, (ii) overpressure during the

discharge process, and (iii) remaining losses of the compression cycle. Diniz et al. (2018) adopted the same approach, except that they dealt with the energy rates and separated the remaining losses into suction superheating and "others". In the view of the authors, the latter term would account for leakage and heat transfer during the expansion and compression processes and cylinder heat transfer during the suction process. Posch et al. (2018) proposed an alternative approach based on the formulation of the second law of thermodynamics, describing the compressor losses in terms of entropy generation and exergy losses.

In the present study, we propose to detachment of the thermodynamic losses following the first law of thermodynamics, replacing the ordinary "process-oriented" approach by an "energy transfer-oriented" one. The applicability of this technique is demonstrated with a theoretical comparative analysis of two reciprocating compressors applied for household refrigeration. Both compressors have the same geometric characteristics, but differ in how the compression chamber volume changes with time. In the first one, a sinusoidal piston displacement is produced by a crank-rod mechanism, while in the second one an optimized piecewise linear piston trajectory is adopted. Prior to the aforementioned analysis, we describe and validate the comprehensive compressor simulation model employed in this study.

2. COMPRESSOR SIMULATION MODEL

The compressor simulation model is based on an unsteady-state lumped-parameter formulation of the mass and energy conservation equations applied to the compression chamber (Bradshaw *et al*., 2011; Engel and Deschamps, 2019), leading to:

$$\frac{dm}{dt} = \dot{m}_s - \dot{m}_{sb} - \dot{m}_d + \dot{m}_{db} - \dot{m}_l + \dot{m}_{lb} \ , \tag{1}$$

$$\frac{dU}{dt} = \dot{Q} - \dot{W} + \dot{m}_s h_{sc} - \dot{m}_{sb} h - \dot{m}_d h + \dot{m}_{db} h_{dc} - \dot{m}_l h + \dot{m}_{lb} h_{ie} \ . \tag{2}$$

In these equations, m is the mass and U is the internal energy of the gas in the compression chamber, t is the time and $\dot{Q}$ is the instantaneous heat transfer rate. The instantaneous compression power is $\dot{W} = p\, dV/dt$, p being the pressure and V the volume of the gas. The variations of kinetic and potential energy wee neglected. The mass flow rates entering and leaving the compression chamber are represented by $\dot{m}$ in which the subscripts s, d and l stand for flow through the suction and discharge ports and leakage through the piston-cylinder gap, whereas sb, db and lb denote backflow through the same passages, respectively. The variable h stands for the specific enthalpy of the gas in the compression chamber whereas h_{sc}, h_{dc} and h_{ie} refer to the specific enthalpies at the suction chamber, discharge chamber and internal environment, which is occupied by gas at low pressure. These equations are integrated using the Euler explicit method and the required thermodynamic properties are evaluated using the thermodynamic properties library CoolProp (Bell *et al*., 2014). Figure 1 presents a schematic of the compression chamber.

The flow of gas through the suction and discharge orifices are modeled assuming a one-dimensional isentropic compressible flow through a nozzle, that is,

$$\dot{m}_i = C_{ee,i} A_i p_{up} \sqrt{\frac{2\gamma}{(\gamma-1)RT_{up}} \left(\Pi^{\frac{2}{\gamma}} - \Pi^{\frac{\gamma+1}{\gamma}} \right)} , \tag{3}$$

where $\dot{m}_i$ stands for the direct or reverse flow through the orifice, A_i is the orifice area, $C_{ee,i}$ is the effective flow area coefficient, γ is the specific heat ratio, R is the specific gas constant and $\Pi = p_{down}/p_{up}$ is the pressure ratio, which is limited to

$$\Pi = \left(\frac{2}{\gamma+1} \right)^{\frac{\gamma}{\gamma-1}} \tag{4}$$

for choked flow condition. The subscripts up and $down$ indicate variables evaluated at the upstream and downstream thermodynamic states, respectively. The effective flow area coefficient is a correction parameter to account for the real flow restriction imposed by the orifice and valve geometry, which is normally obtained from experiments or CFD simulations. Generally, this parameter is described as a function of the valve displacement.

The heat transfer rate between the gas and the walls of the compression chamber is calculated using the Newton's law of cooling:

$$\dot{Q} = HA(T_w - T) \quad , \tag{5}$$

where H is the convective heat transfer coefficient between the gas and the walls, which is obtained from the correlation proposed by Annand (1963). The heat transfer area A includes all surfaces that enclose the gas in the compression chamber. The temperature of the cylinder walls, T_w, is obtained from experimental data and T is the temperature of the gas in the compression chamber.

Additional equations are needed for the valve dynamics, the leakage rate through the piston cylinder gap and the volume of the compression chamber. The valve dynamics is treated as a one-degree-of-freedom mass-spring-damper system, using the concept of effective force areas (Pérez-Segarra *et al*., 2003; Pereira and Deschamps, 2011). The leakage rate through the piston-cylinder gap is calculated assuming an incompressible fully developed laminar flow of pure gas (Ferreira and Lillie, 1984). Finally, the volume of the compression chamber is either imposed by the optimization algorithm or computed from the driving mechanism kinematics equation for a crank-rod compressor (An *et al*., 2002).

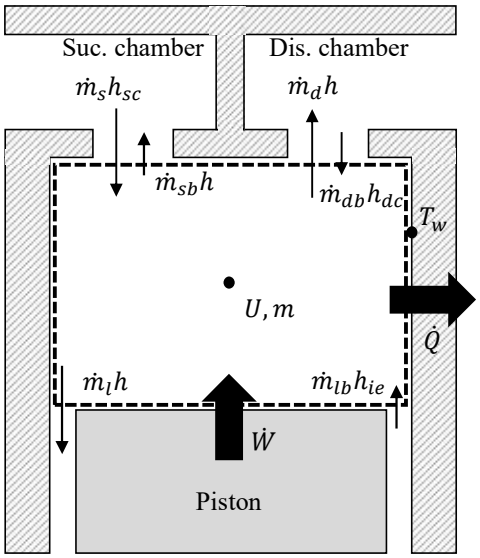

Figure 1. Schematic of the compression chamber.

3. DETACHMENT OF THE THERMODYNAMIC LOSSES

The thermodynamic efficiency is defined as the ratio between the theoretical power $(\dot{W}_{th})$ estimated considering an isentropic process, and the indicated power $(\dot{W}_i)$, obtained from the pressure-volume diagram. Such a definition is also well known in the literature as isentropic efficiency and is expressed as:

$$\eta_t = \frac{\dot{W}_{th}}{\dot{W}_i} = \frac{\dot{m}(h_{d,s} - h_{sc})}{\dot{W}_i} \quad , \tag{6}$$

in which $h_{d,s}$ is the specific enthalpy evaluated with the discharge pressure and the specific entropy of the gas in the suction chamber. The actual mass flow rate $\dot{m}$ is calculated as a function of the instantaneous mass flow rates through the discharge port:

$$\dot{m} = f \int_0^{1/f} (\dot{m}_d - \dot{m}_{db}) dt \ , \tag{7}$$

where f is the operation frequency of the compressor. The indicated power $\dot{W}_i$ is computed as

$$\dot{W}_i = -f \oint p dV \ . \tag{8}$$

The coefficient of performance is a parameter commonly adopted to assess the energetic performance of refrigeration systems and is directly proportional to the thermodynamic efficiency. For this reason, the determination of the main energy losses associated with the compression cycle is paramount. Two approaches are adopted herein to perform this task: (i) one based on the analysis of the indicated diagram and (ii) another derived from the first law of thermodynamics.

3.1 Analysis via the Indicated Diagram

In this traditional approach (Pérez-Segarra et al., 2005), the energy losses due to the suction and discharge processes are computed with reference to ideal isobaric processes at suction line and discharge line pressures p_s and p_d, respectively. In this study, the evaporating pressure p_e is assigned as p_s and the condensing pressure p_c as p_d. Therefore, $\Delta\dot{W}_s$ is estimated by integrating the area of the indicated diagram below the evaporating pressure

$$\Delta\dot{W}_s = -f \oint \min(p, p_s) dV \ , \tag{9}$$

whereas $\Delta\dot{W}_d$ is determined from the area of the indicated diagram above the condensing pressure

$$\Delta\dot{W}_d = -f \oint \max(p, p_d) dV \ . \tag{10}$$

Finally, the energy loss associated with the compression and expansion processes is computed by:

$$\Delta\dot{W}_{ce} = \dot{W}_i - \Delta\dot{W}_s - \Delta\dot{W}_d - \dot{W}_{th} . \tag{11}$$

3.2 Analysis via the First Law of Thermodynamics

By combining Eqs. (1) and (2), the following expression is obtained for the instantaneous compression power:

$$\begin{aligned} \dot{W} = {} & (\dot{m}_d - \dot{m}_{db})\big(h_{sc} - h_{d,s}\big) + (\dot{m}_d - \dot{m}_{db})\big(h_{d,s} - h\big) + \dot{Q} + \dot{m}_l(h_{sc} - h) + \dot{m}_{sb}(h_{sc} - h) \\ & + \dot{m}_{lb}(h_{ie} - h_{sc}) + \dot{m}_{db}(h_{dc} - h) + \frac{dm}{dt} h_{sc} - \frac{dU}{dt} \end{aligned} \ , \tag{12}$$

which is integrated along time for one complete cycle and multiplied by $-f$, yielding

$$\dot{W}_i = \dot{W}_{th} + \Delta\dot{W}_{\dot{Q}} + \Delta\dot{W}_l + \Delta\dot{W}_{lb} + \Delta\dot{W}_{sb} + \Delta\dot{W}_{db} + \Delta\dot{W}_o \ . \tag{13}$$

The terms $\Delta\dot{W}$ are the energy losses due to heat transfer ($\Delta\dot{W}_{\dot{Q}}$), leakage ($\Delta\dot{W}_l$), backflow through the piston-cylinder gap (ΔW_{lb}), backflow through the suction port (ΔW_{sb}), backflow through the discharge port ($\Delta\dot{W}_{db}$) and other losses ($\Delta\dot{W}_o$). All relationships used to calculate the energy losses are presented in Table 1. The term $\Delta\dot{W}_o$ corresponds to the energy loss brought about by the deviation of the gas enthalpy in the compression chamber h with reference to $h_{d,s}$

during the discharge process. Thus, $\Delta\dot{W}_o$ is affected by all losses aforementioned, since they contribute to change the gas enthalpy.

Table 1 – Definition of the energy losses (W).

$\Delta\dot{W}_{\dot{Q}}$	$-f\int_0^{1/f}\dot{Q}dt$	$\Delta\dot{W}_l$	$f\int_0^{1/f}\dot{m}_l(h-h_{sc})dt$	$\Delta\dot{W}_{sb}$	$f\int_0^{1/f}\dot{m}_{sb}(h-h_{sc})dt$
$\Delta\dot{W}_{db}$	$f\int_0^{1/f}\dot{m}_{db}(h-h_{dc})dt$	$\Delta\dot{W}_{lb}$	$f\int_0^{1/f}\dot{m}_{lb}(h_{sc}-h_{ie})dt$	$\Delta\dot{W}_o$	$f\int_0^{1/f}(\dot{m}_d-\dot{m}_{db})(h-h_{d,s})dt$

4. RESULTS

4.1 Compressor Model Validation

Initially, the numerical model was validated against experimental data provided by Diniz et al. (2018) for a compressor with volumetric displacement $V_{sw} = 5.96$ cm^3, operating with R600a at 50 Hz in a household refrigeration system, under on-off cycling conditions. The compression cycle was simulated considering the particular pairs of evaporating and condensing temperatures just before the compressor shut-down for two operating conditions, namely 16B and 32B. The input parameters are shown in Table 2, where T_e, T_c, T_{sc} and T_{dc} represent the evaporating, condensing, suction chamber and discharge chamber temperatures. Due to the lack of information about the thermodynamic state of the gas in the internal environment of the compressor, it was assumed the same as that of the suction chamber. The numerical predictions and experimental data of mass flow rate and indicated power are presented in Table 3. Larger deviations are found for condition 32B, where the numerical predictions of mass flow rate and indicated power are 5.4% and 3.5% lower than the measured ones, respectively. These deviations are acceptable given the simulation model simplicity.

Table 2. Input data for compressor simulation.

Parameter	Condition 16B	Condition 32B
T_e [°C]	-27.1	-24.5
T_c [°C]	31.7	45.6
T_{sc} [°C]	27.0	48.5
T_{dc} [°C]	63.5	92.2
T_w [°C]	42.7	69.9

Table 3. Comparison between measurements and predictions.

Parameter	$\dot{m}$ [kg/h]	$\dot{W}_i$ [W]
	Condition 16B	
Experimental	1.00	29.24
Numerical	0.97	29.37
Deviation	-3.0%	0.4%
	Condition 32B	
Experimental	0.93	34.60
Numerical	0.88	33.38
Deviation	-5.4%	-3.5%

4.2 Thermodynamic Losses Detachment

After the model validation, an optimization procedure was adopted to determine the piston trajectory that maximizes the compressor thermodynamic efficiency under condition 32B, but retaining the baseline volumetric displacement V_{sw}. Valve dynamics was disregarded for the computation of the optimum piston trajectory, which means valves open immediately with the minimum flow resistance when subjected to any positive pressure difference and do not experience backflow. Such an assumption intended to avoid an optimized piston trajectory constrained by any particular set of suction and discharge valves. Moreover, valve design is typically carried out after the driving mechanism is specified, i.e. after the piston trajectory is defined. For comparison purposes, ideal valves were also adopted for the compressor with the crank-rod mechanism. More details about the piston trajectory optimization are described in Silva and Dutra (2021).

Table 4 presents results for the thermodynamic losses detachment using the indicated diagram analysis. All losses are normalized with respect to the theoretical power, $\Delta W^* = \Delta W / W_{th}$. Baseline crank-rod compressor and optimized piston trajectory compressor are denoted by CR and OPT, respectively. The optimization of the piston trajectory brings about a slight increase in the discharge losses, which are overcome by a decrease of losses associated with compression and expansion processes. As a result, the indicated power is reduced and the thermodynamic efficiency increases 3.8% with the OPT configuration (from 88.3% to 92.1%). However, it is not possible to identify the mechanisms behind the compression and expansion processes that are responsible for such an efficiency improvement.

The approach based on the application of the first law of thermodynamics gives a different insight of losses detachment. Table 5 presents the thermodynamic losses for CR and OPT cases obtained from a stratification using the First Law Approach. Note that only heat transfer, piston-cylinder leakage and other losses are included, since leakage backflow is zero ($\Delta\dot{W}_{lb} = 0$) and ideal valves were adopted in this section for both configurations, resulting in no backflow losses ($\Delta\dot{W}_{sb} = \Delta\dot{W}_{db} = 0$). The optimization of the piston trajectory provides a reduction of the energy loss due to the piston-cylinder leakage of 43.0% (from 2.6 W to 1.5 W) and a decrease on the net heat transfer rate by 40.6% (from 2.6 W to 1.6 W) with reference to the CR configuration. Moreover, the term $\Delta\dot{W}_o$ acts as a gain for both OPT and CR, which means that h is lower than $h_{d,s}$ during the discharge process. Such a deviation is larger for the CR (-1.1 W) because heat transfer and leakage losses are also larger for this compressor and they contribute to reduce the gas enthalpy in the compression chamber.

Table 4. Thermodynamic losses detachment Indicated Diagram Analysis / Condition 32B.

Parameter	CR	OPT
$\dot{W}_{th}$ [W]	31.5	32.0
$\Delta\dot{W}_s$ [W] / $\Delta\dot{W}_s^*$[%]	0.1 / 0.3	0.1 / 0.3
$\Delta\dot{W}_d$ [W] / $\Delta\dot{W}_d^*$[%]	0.2 / 0.6	0.6 / 1.9
$\Delta\dot{W}_{ce}$ [W] / $\Delta\dot{W}_{ce}^*$[%]	3.8 / 12.1	2.0 / 6.3
$\dot{W}_i$ [W]	35.6	34.7
η_t [%]	88.5	92.2

Table 5. Thermodynamic losses detachment First Law Approach / Condition 32B.

Parameter	CR	OPT
$\dot{W}_{th}$ [W]	31.5	32.0
$\Delta\dot{W}_{\dot{Q}}$ [W]	2.6	1.6
$\Delta\dot{W}_l$ [W]	2.6	1.5
$\Delta\dot{W}_o$ [W]	-1.1	-0.3
$\dot{W}_i$ [W]	35.6	34.7
η_t [%]	88.5	92.2

It is necessary to analyze the piston trajectory to understand the reasons behind the reduction of leakage and heat transfer losses associated with the OPT. Figure 2 shows the volume of the compression chamber along the compression cycle for both the (a) conventional compressor with a crank-rod mechanism and (b) the optimized compressor. It is interesting to note that the bottom dead center is anticipated in the optimized configuration, which means that the time required to execute the expansion and suction processes is shorter than that comprising the compression and discharge processes. In addition, the expansion and discharge strokes in the OPT case are nearly 50% shorter than those in the CR compressor.

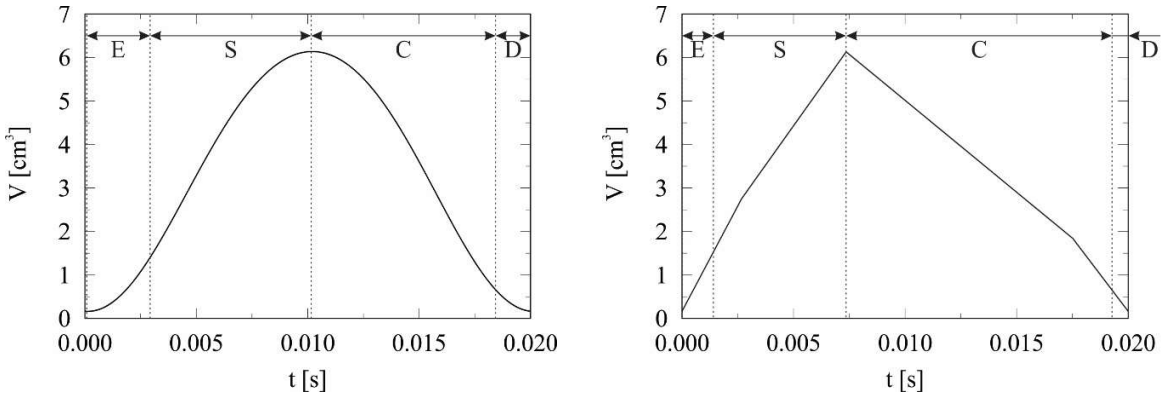

(a) CR (b) OPT

Figure 2. Volume of the compression chamber (V) as a function of time (t). E: expansion, S: suction, C: compression, D: discharge.

The thermodynamic losses assessed via the First Law Approach are normalized with respect to the theoretical power and detached into the four strokes of the compression cycle, as shown in Fig. 3. There is an increase in the heat transfer losses related to the compression stroke in the OPT case, since the time required to carry out this process is 43% longer than that observed in the CR mechanism (Fig. 2). However, the decrease in the thermodynamic losses associated with the expansion and the discharge processes of the optimized configuration overcomes the increase in the compression process losses, leading to a gain in terms of thermodynamic efficiency.

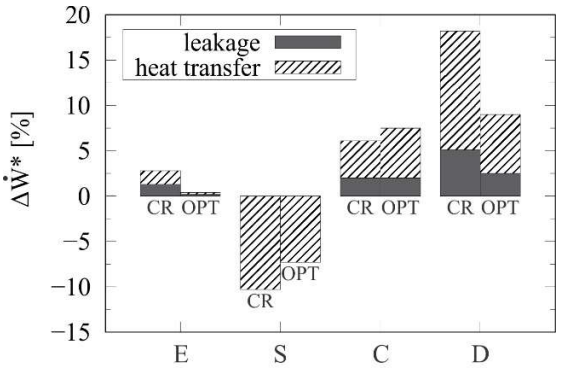

Figure 3. Normalized energy losses along different processes.

5. CONCLUSION

This paper presented an approach to assess the thermodynamic losses of a reciprocating compressor based on the application of the first law of thermodynamics. For this purpose, a compressor simulation model based on a transient and lumped formulation of mass and energy conservation equations applied to the compression chamber was developed and validated with experimental data. A study case was performed in which the thermodynamic losses of a baseline compressor was compared with those of an optimized piston trajectory compressor. Loss assessment based on the indicated diagram analysis indicates the efficiency of the optimized piston trajectory compressor increases nearly 4% due to the reduction of losses associated with compression and expansion processes, but the mechanisms that lead to such a loss reduction are not identified. By applying the First Law Approach, we found out that the optimized piston trajectory led to reductions of 43.0% and 40.6% in the piston-cylinder leakage and heat transfer losses, respectively, which were due to 50% shorter expansion and discharge processes with respect to the baseline crank-rod compressor. Although the First Law Approach have been presented for a reciprocating compressor, it can be extended to other compressor types, such as rotary and scroll.

NOMENCLATURE

A	area	(m^2)	**Subscript**	
f	frequency	(Hz)	*c*	condensing
h	specific enthalpy	(J/kg)	*d*	discharge
H	convective heat transfer coefficient	($W/m^2.K$)	*db*	discharge backflow
m	mass	(m)	*dc*	discharge chamber
$\dot{m}$	mass flow rate	(kg/s)	*e*	evaporation
p	pressure	(Pa)	*i*	Indicated
$\dot{Q}$	heat transfer rate	(W)	*l*	Leakage
t	time	(s)	*lb*	leakage backflow
T	temperature	(°C)	*o*	Other
V	volume	(m^3)	$\dot{Q}$	heat transfer
V_{sw}	volumetric displacement	(m^3)	*s*	isentropic, suction
$\dot{W}$	power	(W)	*sb*	suction backflow
U	internal energy	(J)	*sc*	suction chamber
$\Delta\dot{W}$	thermodynamic loss	(W)	*t*	Thermodynamic
$\Delta\dot{W}^*$	normalized thermodynamic loss	(-)	*th*	theoretical
η	efficiency	(-)	*W*	cylinder wall
ρ	density	(kg/m^3)		

REFERENCES

An, K.H., Lee, J.H., Lee, I.W., Park, S.C. (2002). Performance prediction of reciprocating compressor. *In: Proc. Int. Compressor Eng. Conf. at Purdue*, West Lafayette, Paper 1525.

Annand, W.J.D. (1963). Heat transfer in the cylinders of reciprocating internal combustion engines. *Proc. Instn. Mech. Engnrs*., 117, pp. 973-996.

Bell, I.H., Wronski, J., Quoilin, S., Lemort, V. (2014). Pure and pseudo-pure fluid thermophysical property evaluation and the open-source thermophysical property library coolprop. *Ind. Eng. Chem. Res.,* 53 (6), pp. 2498-2508.

Bradshaw, C.R., Groll, E.A., Garimella, S.V. (2011). A comprehensive model of a miniature-scale linear compressor for electronics cooling. *Int. J. Refrigeration*, 34, 63-73.

Coulomb, D., Dupont, J.L., Pichard, A. (2015). The role of refrigeration in the global economy. 29th Informatory Note on Refrigeration Technologies, *Technical Report, International Institute of Refrigeration*: Paris, France.

Diniz, M.C., Melo, C., Deschamps, C.J. (2018). Experimental performance assessment of a hermetic reciprocating compressor operating in a household refrigerator under on–off cycling conditions. *Int. J. Refrigeration*, 88, 587-598.

Engel, R.C., Deschamps, C.J. (2019). Comparative analysis between the performances of reciprocating and rolling piston compressors applied to a domestic heat pump water heater. *Int. J. Refrigeration*, 102, 130-141.

Ferreira, R.T.S., Lillie, D.E.B. (1984). Evaluation of the leakage through the clearance between piston and cylinder in hermetic compressors. *In: Proc. Int. Compressor Eng. Conf. at Purdue, West Lafayette*, Paper 424.

Pereira, E.L.L, Deschamps, C.J. (2011). Influence of piston on effective areas of reed-type valves of small reciprocating compressors. *HVAC&R Res*., 17:2, 218-230.

Pérez-Segarra, C.D., Rigola, J., Sòria, M., Oliva, A. (2005). Detailed thermodynamic characterization of hermetic reciprocating compressors. *Int. J. Refrigeration*, 28, 579-593.

Pérez-Segarra, C.D., Rigola, J., Oliva, A. (2003). Modeling and numerical simulation of the thermal and fluid dynamic behavior of hermetic reciprocating compressors-part 1. *HVAC&R Res*., 9:2, 215-235.

Posch, S., Hopfgartner, J., Dürr, L., Eichinger, M., Stangl, S. & Almbauer, R. (2018). Thermal loss analysis of hermetic compressors using numerical simulation. *Appl. Therm. Eng.,* 130, 1580–1589.

Silva, E., Dutra, T. (2021). Piston trajectory optimization of a reciprocating compressor. *Int. J. Refrigeration*, 121, 159-167.